Journal of Power Sources 260 (2014) 186–196

Contents lists available at ScienceDirect

Journal of Power Sources

journal homepage: www.elsevier.com/locate/jpowsour

Review

Co-laminar flow cells for electrochemical energy conversion

Marc-Antoni Goulet, Erik Kjeang*

School of Mechatronic Systems Engineering, Simon Fraser University, 250-13450 102 Avenue, Surrey, BC V3T 0A3, Canada

HIGHLIGHTS

- Categorization and standardization of co-laminar flow cell technology is proposed.
- The technology is gaining importance as an analytical and educational platform.
- Practical, competitive power density levels are demonstrated.
- Emerging rechargeable 'membraneless' flow batteries are discussed.
- Recommendations for further research are provided.

GRAPHICAL ABSTRACT

This review discusses the recent trends and opportunities in the use of co-laminar flow of reactants as an alternative to membranes for power generating electrochemical cells.

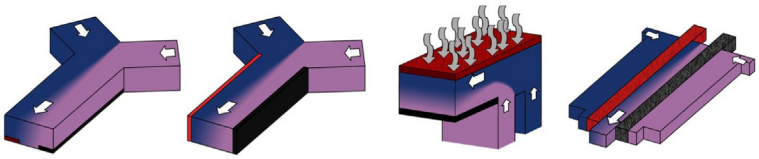

ARTICLE INFO

Article history:
Received 22 January 2014
Received in revised form
24 February 2014
Accepted 5 March 2014
Available online 29 March 2014

Keywords:
Laminar flow
Microfluidic
Fuel cell
Flow battery
Energy storage
Energy conversion

ABSTRACT

In this review, we present the major developments in the evolution of 'membraneless' microfluidic electrochemical cells which utilize co-laminar flow to minimize reactant mixing while producing electrical power in a compact form. Categorization of devices according to reactant phases is suggested, with further differentiation being subject to fabrication method and function, namely multi-layer sandwich structures for medium-power cell stacks and single-layer monolithic cells for low-power on-chip applications. Power density metrics reveal that recent co-laminar flow cells compare favourably with conventional membrane-based electrochemical cells and that further optimization of device architecture could be expedited through standardized testing. Current research trends indicate that co-laminar flow cell technology for power generation is growing rapidly and finding additional use as an analytical and education tool. Practical directions and recommendations for further research are provided, with the intention to guide scientific advances and technology development toward ultimate pairing with commercial applications.

1. Introduction

Chemical energy storage has been the method of choice for portable power applications due its high specific energy [1]. Electrochemical energy conversion is considered galvanic when the chemical energy of two half-cell reactions is converted into electrical energy, whereas it is electrolytic when electricity is used to produce species of higher chemical energy in the reverse process [2]. Historically, the term fuel cell has been applied to any galvanic electrochemical cell which converts the chemical energy of a fuel and oxidant combination directly into electrical energy [3]. More recently, the term redox flow battery (RFB) has become popular to describe electrochemical cells which utilize two redox couples dissolved in separate liquid electrolytes as the fuel and oxidant [4]. As thermodynamically open systems, both of these electrochemical flow cells can be instantly recharged with new reactants, a desirable property which eludes conventional closed-cell batteries and may offer a potential solution to the growing demand for compact energy supplies for portable electronics and a host of other low-power applications [1]. Occasionally, fuel cells have been used for

* Corresponding author. Tel.: +1 778 782 8791; fax: +1 778 782 7514.
E-mail address: ekjeang@sfu.ca (E. Kjeang).

http://dx.doi.org/10.1016/j.jpowsour.2014.03.009
0378-7753/

the reverse electrolytic process of recreating the same fuel and oxidant combination by applying an external potential, such as the regenerative systems developed by NASA for long term space missions [5]. Since reactants often undergo phase changes during charge and discharge, these regenerative fuel cells typically suffer from low cycle efficiency due in part to the difficulty of optimizing the structure for both directions of phase change. Essentially operating as continuously recirculating regenerative fuel cells, rechargeable RFBs on the other hand do not suffer from phase change issues and can therefore be conveniently optimized to achieve high cycle efficiencies up to 80% [6].

Regardless of terminology, most modern electrochemical flow cells employ polymer electrolyte membranes to separate the reactants while maintaining the ionic conductivity necessary to complete the circuit. These specialized solid state ionomer membranes are designed to allow either hydrogen ions in acidic conditions or hydroxide ions in alkaline conditions to pass while preventing the crossover of other chemical species. Recent ionomer membrane development has contributed to significant reductions in film thickness, with 25–50 μm being a typical thickness used in hydrogen fuel cells [7] and 125 μm being used in vanadium redox batteries [8]. Although this trend has led to significant performance gains due to reduced ionic resistance, it has also led to certain technical challenges. In the case of hydrogen fuel cells, thinner membranes tend to degrade and rupture more quickly leading to cell failure [9]. In the case of direct methanol fuel cells (DMFC), typical membranes still allow considerable crossover of methanol fuel due to diffusion and electro-osmotic drag [3]. It has also been observed that rates of vanadium redox species crossover in ionomer membranes are different for each ion which eventually imbalances the concentrations of fuel and oxidant, requiring rebalancing of the entire vanadium redox battery [4,10]. In addition to durability and crossover issues, polymer electrolyte membranes considerably increase the cost of electrochemical cells, particularly for alkaline fuel cells which require more expensive hydroxide-permeable anion exchange membranes [11]. Current membrane electrode assembly (MEA) designs are also inadequate for monolithic integration into miniaturized devices [1].

For all of the above reasons, many alternatives have been sought to replace or improve existing polymer electrolyte membranes. Recent advances in the field of microfluidics and nanofluidics enable promising opportunities to eliminate the membrane through hydrodynamic engineering. At the microscale, fluid dynamics is typically characterized by low Reynolds numbers ($Re < 10$) which indicates smooth laminar flow free of chaotic turbulence. This phenomenon permits two laminar streams to flow side by side with mixing occurring only by cross-stream diffusion. Several studies have explored the practical application of this phenomenon for DNA analysis [12], molecular positioning [13], microfluidic switches [14], and a wide range of other applications [15]. It was proposed in 2002 that stratified co-laminar flow of two electrochemical reactant streams would allow for ionic conduction while maintaining reactant purity, thereby replacing the costly membrane [16,17]. Such 'membraneless' cells were first demonstrated in 2002, and have been the subject of numerous other studies since.

A detailed and comprehensive review of all types of microfluidic fuel cells was published by Kjeang et al. in 2009 [18]. Since then, the research in this field has not only evolved substantially in the core technical area of microfluidic fuel cells, but has also ventured into the domain of rechargeable batteries. A critical juncture has been reached, where technology pairing with practical, commercial applications is essential for effective further development. The purpose of the present review article is to highlight notable advancements in the field since 2009 and to extract the key historical trends in the rapid development of electrochemical cells based on co-laminar flow technology. These trends are then used to offer a forward-looking, pragmatic perspective on the advantages and disadvantages of this technology and provide practical directions for future work. The focus of this review is strictly on co-laminar flow cells and the scope does not include other types of microfluidic cells as reviewed elsewhere [18–20].

2. Design evolution

The advent of microfluidics has opened up the door for a variety of non-conventional electrochemical cell architectures that do not require a membrane. The most fundamental co-laminar flow cell design is illustrated schematically in Fig. 1. The design features stratified co-laminar flow of fuel and oxidant in supporting electrolyte through a shared microfluidic channel with electrodes positioned on the walls.

2.1. Design constraints

While the electrochemical reactions and electrode materials are generally consistent with those of conventional electrochemical cells, the membraneless function of co-laminar flow cells has certain requirements on the cell design. Firstly, the flow must be laminar to prevent turbulent mixing of the two streams, which is facilitated by low Reynolds numbers ($Re < 1000$) [21]. Secondly, the residence time t_{res} in the electrochemical chamber must be shorter than the diffusion time t_{diff} for crossover of a reactant species to the opposite electrode in order to avoid a mixed potential. In this situation, the thermodynamic potential difference between the two electrodes would follow the same Nernst relation [2] as any other electrochemical cell with identical reactants. This necessary criterion can

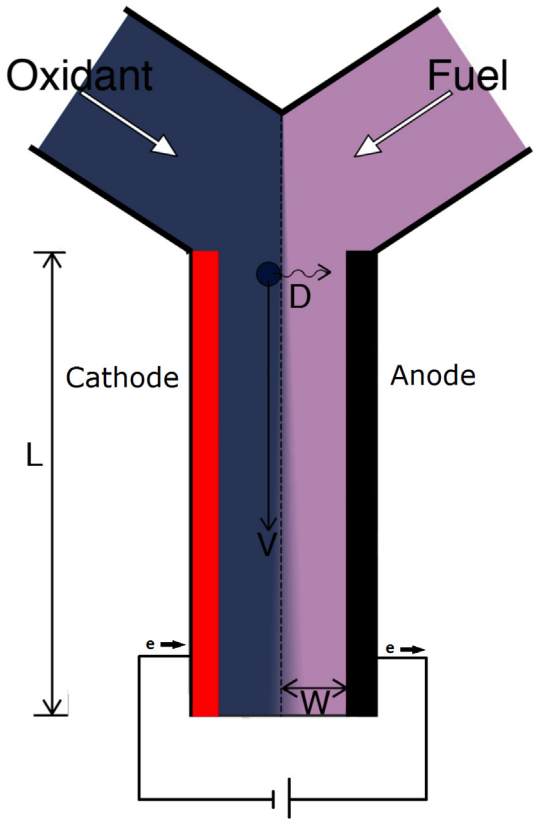

Fig. 1. Schematic of co-laminar flow cell operation.

be estimated using Einstein's relation for one-dimensional Brownian diffusion [22], as a lower bound on the average diffusion time:

$$t_{res} = \frac{L}{v} < \frac{W^2}{2D} = \overline{t_{diff}} \quad (1)$$

The above equation includes two design parameters, namely the channel length L and width W (the mean diffusion distance), the mean velocity v as an operational parameter, and the diffusion coefficient D of the reactant species. Experimentally, the velocity is controlled indirectly by the flow rate Q and is itself a function of the channel height H and width W. These additional constraints can be included to obtain the following dimensionless relation for the ratio of solute (reactant) advection to cross-stream diffusion in co-laminar flow cells:

$$\frac{QW}{2DHL} > 1 \quad (2)$$

A similar design rule to the one in Eq. (2) can also be derived for this geometry from the Péclet number [21], which is the ratio between advective flux and diffusive flux. From this point of view, the above relation holds when the rate of downstream advective transport exceeds the rate of reactant crossover towards the opposite electrode. As the above relation is derived for an average diffusion time, it is recommended for the ratio to exceed 1 by an appreciable margin. For example, in order achieve a suggested minimum ratio of 10 for a species with a $\sim 10^{-10}$ m^2 s^{-1} diffusion coefficient in a 0.5 mm high, 0.5 mm wide and 10 mm long channel, the required flow rate would be on the order of ~ 1 μL min^{-1}. Finally, cell designers must also consider the finite ionic conductivity of the supporting electrolyte in the context of the channel dimensions to minimize ohmic losses as well as the parasitic pumping power requirements to drive the flow in various channel dimensions. Ideally, these stipulations could be added to the analytical expression derived above and explored through numerical modelling to determine the optimum design and operational parameters. Typically, micro-channels with ~μL to ~mL per minute flow rates generally provide an optimum balance with respect to the above mentioned constraints. Therefore, co-laminar flow cells are often termed 'microfluidic' cells.

2.2. Architecture and fabrication

Many variations on the original co-laminar flow concept presented in Fig. 1 have been developed in the past 10 years. The schematic illustrations provided in Fig. 2 represent the key conceptual developments which have generated significant traction in this field to date. Although all of these designs establish co-laminar flow of two separate electrolytes, they differ either in their architecture or their fabrication method. The first co-laminar flow based fuel cell published by Ferrigno et al. (Fig. 2a) was a simple Y-junction microfluidic channel with two inlets and a single outlet [16]. The device was constructed using soft-lithography of poly(-dimethylsiloxane) (PDMS), a method used for many other microfluidic applications. The electrodes themselves, otherwise known as planar 'flow-by' electrodes, were deposited on the bottom of the centre channel and were therefore perpendicular to the co-laminar flow interface during operation. With both the electrodes and the microfluidic channels being part of the same layer, this single-layer monolithic cell has the potential to be integrated into on-chip systems and other MEMS devices [23]. Whether the junction is Y-shaped or T-shaped, this monolithic device platform has spawned many derivative studies [24–38] due to its simple implementation and operation, and has been particularly favoured by several research groups investigating potential biofuel cell applications with microbial or enzymatic catalysts [29,30,36–38].

Another device (Fig. 2b), developed around the same time by Choban et al. [17], featured a multi-layer sandwich construction which used two electrode surfaces separated by an insulating spacing layer and sealed between two additional plates to form the microfluidic channel. The 'flow-by' electrodes were therefore positioned parallel to both the flow and the co-laminar interface. This type of multi-layer co-laminar cell [17,39–50] has evolved considerably since this time and many cells now resemble the high aspect ratio conventional membrane electrode assembly (MEA) of existing polymer electrolyte fuel cells [50]. While these cells benefit from a low cost of fabrication requiring no lithography infrastructure and a simplified design which is more amenable to stacking, they may suffer from limited compatibility with on-chip integration and reduced visibility of the co-laminar interface.

Following directly from this work, it was later proposed by Jayashree et al. that the multi-layer device layout could be converted to an air-breathing cell by using a blank stream of electrolyte flowing by a gas diffusion electrode (GDE) as the cathode [51]. By replacing one of the graphite plates with a porous hydrophobic GDE, the reduction reaction could utilize oxygen from the surrounding ambient air or a dedicated stream of oxygen gas, as depicted in Fig. 2c. Although the inlets could potentially be positioned to form a Y-junction [52,53], the F-shaped junction with the inlets on the same side has most often been used [51,54–58], which results in one electrolyte cradling the other until they both exit through a common outlet. The concept of air-breathing electrode was adapted from conventional electrochemical cells such as polymer electrolyte fuel cells [59] or metal-air batteries [60] and innovatively applied to the microfluidic co-laminar fuel cell. Due to the requirement of a blank electrolyte stream, there is no net energy density advantage as for the other technologies; however, the demonstrated and repeated results establish the viability of the concept should it become desirable.

In 2008, Kjeang et al. demonstrated that the reactant streams coming from the inlets could be passed through porous electrodes and still maintain a co-laminar interface until reaching the outlet [61]. These 'flow-through' porous electrodes depicted in Fig. 2d largely eliminated reactant depletion issues at the electrodes and therefore maximized the fuel utilization. Using the same lithographic process as the original Y-junction cell to form the microfluidic channels, the porous electrodes were simply placed in their positions and lightly compressed by the glass capping layer to

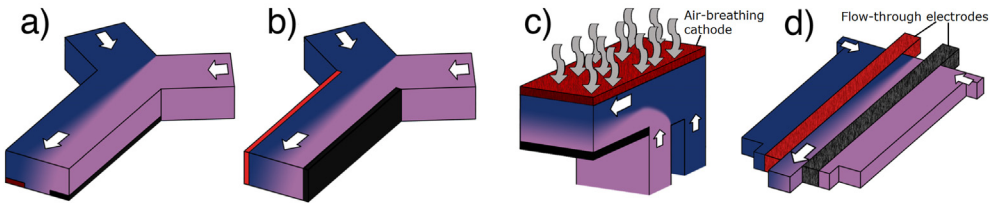

Fig. 2. Primary co-laminar flow cell developments: a) monolithic flow-by cell; b) multi-layer flow-by cell; c) air-breathing flow-by cell; and d) monolithic cell with flow-through electrodes.

retain the monolithic device structure. Although several studies [62–66] have since used the same baseline design, it has been demonstrated that porous flow-through electrodes can also be implemented with the multi-layer construction method [53,67].

Additional co-laminar flow cell architectures and fabrication methods besides those featured in Fig. 2 have been proposed, such as the innovative radial distribution cell by Salloum et al. [68], or the dual-pass concept published by our group [69], but neither of these have yet received as much attention or engendered secondary studies.

2.3. Modelling

The development of co-laminar flow cells can benefit substantially from computational and theoretical models that are capable of predicting the performance of different cell designs and can be employed to guide prototyping of new devices. In general, practical simulation of co-laminar flow cell operation requires coupled solving of the conservation equations for mass, momentum, species, and charge, convective–diffusive transport, and electrochemical reactions. Highlighted here are the trends and recent contributions in co-laminar flow cell modelling, whereas the reader is referred to a recent, detailed review by Nasharudin et al. which summarizes most of the noteworthy modelling contributions in this field [70]. Among all the modelling studies [48,49,71–104] published to date, the majority have considered the Y-junction geometry with planar flow-by electrodes. Some of the first contributions focused on the depletion boundary layer which forms at the electrode surface in the case of slow cross-stream diffusive transport in the laminar flow combined with relatively rapid electrochemical kinetics [71,73–75,78]. A study by Yoon et al. suggested the use of multiple inlets or outlets to replenish the reactants [49]. Several other studies have explored strategies to minimize diffusion based crossover of reactant species with the most common suggestion being to taper the electrodes away from the co-laminar interface, thereby increasing the length required for crossover [71], or to taper the channel downstream to increase the convective velocity of the electrolyte [49,97]. More recent works have analysed the performance of the air-breathing cell design [84,87,99,100,103], with the study by Xuan et al. in 2013 demonstrating that this design will eventually be limited by oxygen starvation when the anode performance exceeds 200 mA cm^{-2} [103]. Due to the added computational and experimental complexity, only two studies on flow-through porous electrodes were published to date [90,102]. In particular, the recent study by Sprague et al. suggests the use of nanoporous electrodes to increase the advective flux within the electric double layer [102]. Regardless of the geometry chosen, many of the recommendations emerging from the various modelling studies have yet to be implemented into a working device and verified experimentally.

2.4. Recent developments

The established co-laminar flow cells featured in Fig. 2 constitute the most important developments in ‘membraneless’ co-laminar flow cell design to date but do not represent an exhaustive list of all developments of the technology. Several new research trends can be identified from the literature. Recently, several experimental contributions have demonstrated advances in terms of reactant crossover mitigation and mass transport enhancement by utilizing non-uniform cross-sectional channel geometries [31,98,105]. For example, Park et al. showed that an H-shaped centre channel configuration may increase the current density of the cell. Another strategy to minimize diffusive mixing is the use of porous separators between streams, which can allow for reduced crossover and mixing or enlarged electrochemical chamber dimensions beyond those prescribed by the co-laminar interface alone [106–110]. Although the non-selective separators used in most of these studies do not suffer from the same cost and durability drawbacks as a typical ionomer membrane, they do serve essentially the same purpose. It is possible that the combination of co-laminar flow with an added convective barrier may be sufficient to enable scale-up of individual cells for medium-power applications.

Other recent efforts to increase the power density of co-laminar flow cells have focused largely on electrode and catalyst materials. For flow-over electrodes, various carbon supports such as multi-walled carbon nanotubes have been used in conjunction with noble metal catalysts such as gold and palladium for both glucose and formic acid oxidation [25,32,47,111]. Although these electrochemical studies were targeted toward co-laminar flow cells in particular, their results are widely applicable to more conventional cells utilizing these reactants. For cells with flow-through electrodes, the current density can be improved either by addition of catalysts or by application of nanoporous electrodes. A study by Lee et al. demonstrated improved performance over previous designs by replacing carbon paper with carbon nanofoam [66]. Although smaller pore sizes generally favour faster reactant replenishment and may even eliminate the depletion boundary layer within the electrodes entirely, this inevitably leads to greater power loss due to the added pumping pressure required. Apart from the modelling results previously mentioned by Sprague et al. [102], a systematic study of such pros and cons on the efficiency of co-laminar flow cells has yet to be performed.

It is important to note that many supplementary contributions have been made in this field without the express purpose of modifying the design to improve performance of single cells. For instance, two recent contributions have addressed the challenges associated with stacking of microfluidic electrochemical cell devices without disrupting the physics and quality of the co-laminar flow [63,112]. Another emerging trend in this field is the development of microfluidic biofuel cells, where metallic catalysts are replaced by bio-electrocatalytic enzymes or microbial cells. For biofuel cells, the microfluidic channels created by lithography are an ideal starting point for immobilization of biological catalysts [29] and potential integration with miniaturized biomedical devices [45].

Until very recently, nearly all of the research on co-laminar flow cells has focused on single pass fuel cell operation. Most cells have been designed with a single outlet leading to the unavoidable mixing of unused reactants, thereby preventing further recirculation. When operated below 100% fuel utilization conditions, this limits the overall energy efficiency of the cells. Recent work by our group proposed a novel symmetric dual-pass architecture, shown in Fig. 3, which splits the co-laminar streams to allow for fuel recirculation [69,113]. The performance and reactant crossover of this architecture was recently characterized by our group and compared with a more straightforward Y-junction architecture [114]. In this study, it was shown that although both architectures are capable of fuel reutilization, the dual-pass architecture is typically prone to higher diffusion but also higher power output. The microfluidic redox battery (MRB) published in 2013, which is a 2nd generation of the symmetric co-laminar flow cell shown in Fig. 3, was custom-designed to minimize this diffusion at the splitting point of the streams. With these design improvements, the cell demonstrated the capability to serve as the first rechargeable redox flow battery with ~20% full cycle energy efficiency [69]. Later that year, another membraneless flow battery based on the co-laminar flow of bromine and hydrobromic acid with a hydrogen breathing anode was published by Braff et al. [115,116], demonstrating record setting power density and further highlighting the usefulness of the co-laminar concept for both fuel cells and flow batteries.

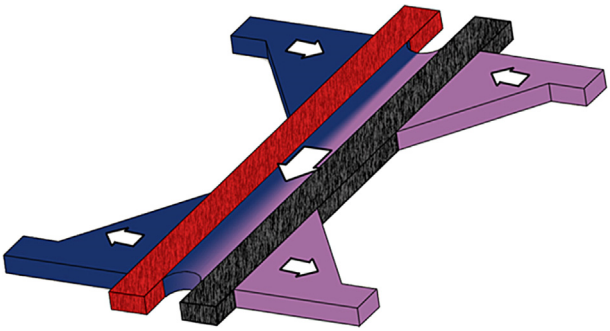

Fig. 3. Symmetric and monolithic co-laminar flow cell for fuel recirculation and regeneration, otherwise known as microfluidic redox battery [113].

As the development of co-laminar flow cells progresses, it will be these types of design improvements that will eventually demonstrate whether the technology is commercially viable. More specifically, architectural modifications are likely to be made according to performance or functionality requirements whereas fabrication modifications would address issues related to cost, scale-up, and device integration.

3. Categorization

Flow cells designed for electrochemical energy conversion include both fuel cells and redox flow batteries. Traditionally, fuel cells have been classified by their electrolyte material such as polymer electrolyte PEFCs or solid oxide SOFCs [3]. Hence, fuel cells which rely on microfluidic co-laminar streams as an electrolyte interface have interchangeably been called microfluidic fuel cells (MFCs) or the bulkier but more descriptive name of laminar flow fuel cells (LFFCs) since the emergence of the field. As technologies evolve, however, further differentiation becomes unavoidable. For instance, within the category of PEFCs there exists the subcategory of direct methanol fuel cells (DMFCs). Similarly, co-laminar flow cells may need to be further subdivided in order to be judged appropriately. In the case of fuel cells mentioned above, their distinction comes from their intended purpose and the physical properties of their reactants which impose certain design constraints. For the same reason, it was recently proposed by our group [20] that microfluidic fuel cells be categorized by the phases of their respective fuels and oxidants since this will eventually determine their fundamental physics and become the limiting factor in their architectural design, making direct performance comparisons more meaningful. Any further differentiation is likely to stem from engineering or fabrication considerations according to the following two application-oriented subgroups: planar monolithic types for low-power on-chip applications; and stacked multi-layer types for medium-power device integration.

3.1. Liquid/liquid reactants

The first, most prevalent and convenient form of co-laminar flow cell utilizes two liquid phase reactants. A variety of liquid fuels have been used, including dissolved hydrogen [42] , methanol [39,40,50,55,56,58,98], formic acid [17,31,32,41,44,46,47,51,52,54,56,57,117,118], hydrogen peroxide [26,28], V^{2+} [16,27,61,62,65,67,69,106,112,119], glucose [25,37,38,45,120–122], glycerol [43], acetate [123], sodium borohydride [56,108], hydrazine and ethanol [56]. The most commonly used oxidants are dissolved oxygen [17,39–42,46,117], hydrogen peroxide [26,46], VO_2^+ [16,27,61,62,65,67,69,106,112], and potassium permanganate [28,35,62,68].

One advantage of the co-laminar interface over the traditional membrane is the inherent compatibility with both acidic and alkaline supporting electrolyte conditions. Traditional electrolyte membranes are designed to conduct either hydrogen or hydroxide ions and cannot operate effectively in both alkaline and acidic media [124]. On the other hand, it was first demonstrated by Cohen et al. that co-laminar flow cells can operate with such a pH gradient [42]. This allows the pH to be tailored to maximize the potential of each electrode reaction independently, and boost the overall cell voltage. Other experimental contributions with mixed media conditions include those by Choban et al. [39] and Hasegawa et al. [26].

A common problem in all-liquid microfluidic systems, the formation of bubbles within a microchannel is often sufficient to disturb the co-laminar interface and increase reactant crossover, reduce ionic conductivity, or block the channel completely [34]. Even with liquid reactants it is possible to form gaseous products with certain fuel and oxidant combinations. If such combinations are desired, reliable strategies must be developed to accommodate gaseous products. At low current densities, dissolution of gas bubbles within the liquid electrolytes may be sufficient to remove the reaction products without compromising the co-laminar flow. At higher current densities, bubble formation can potentially be captured in grooved microchannels to minimize the disturbance [28]. In a recent study by Hur et al. [125], it was proposed and demonstrated that bubbles can be used to drive the capillary flow of electrolytes. In either case, however, gaseous products require increased system complexity and lead to decreased performance stability and therefore may not be warranted due to the availability of alternative reactants.

3.2. Liquid/gaseous reactants

As explained above, it was demonstrated by Jayashree et al. [51] that the concept of an air-breathing cathode could be applied to co-laminar flow cells, resulting in a liquid fuel and gaseous oxidant combination. Other developments involving the air-breathing design have been performed by Shaegh et al. with the added feature of using a flow-through anode [53]. In both cases, the multi-layer fabrication method seen in Fig. 2(b,c) is preferred over the planar lithographic fabrication method due to the relative ease of incorporating a GDE into a sandwich structure. In either case, however, two electrolyte streams are necessary and therefore most standard channel structures (Fig. 2) could potentially be converted into an air-breathing cell. It should also be noted that hydrogen-breathing cathodes have also been attempted by Braff et al. with a liquid bromine anode [116]. Although the liquid/gaseous design requires the same number of manifolds to distribute the electrolytes and gain the same mixed media opportunities, it warrants a separate classification. The reason for distinguishing the liquid/gas design is due to the constraint on the gaseous electrode to have a well-defined triple-phase interface between the liquid electrolyte, the gaseous oxidant, and the solid-state electrode material, in contrast to the regular electrolyte/electrode interface which allows for flow-through electrodes to be fully utilized. Moreover, the need for gas access will inevitably lead to different design constraints for scale-up, pressure control, and device implementation, similar to MEA based liquid/gaseous electrochemical cells. For instance, monolithic device integration of gaseous electrodes is challenging, and poses constraints on fabrication process compatibility and miniaturization opportunities.

4. Comparison

As previously explained, the novelty behind co-laminar flow cells is a particular architecture which permits the usual ionomer

membrane to be replaced by a co-laminar interface of two flowing electrolytes. Although common performance measurements can be made on all devices, direct comparisons between different cell architectures are difficult due to several confounding factors. The following subsection compares the leading co-laminar flow fuel cells in each category according to several common and proposed performance metrics. Subsequently, it is discussed why isolated performance comparisons may not holistically reflect the advantages or drawbacks of each cell design, and a few recommendations for future comparative work are offered.

4.1. Performance

Ever since the development of the modern membrane electrode assembly (MEA), the most commonly cited performance metrics for traditional fuel cells are the peak power of the entire cell and the peak power density normalized by the geometric electrode area [126]. The power density convention was defined to compare single cells with different size, since the current and therefore the power theoretically scales in direct proportion to the electrode surface area. This convention is difficult to adapt to the liquid electrolyte interface of co-laminar flow cells which is only practical at certain length scales. Nevertheless, most co-laminar flow cells utilizing planar electrodes continue to follow the power density convention according to the geometric area of a single electrode. In the case of flow-through porous electrodes, performance normalization was initially reported using the projected electrode area, while more recent studies reported densities based on the cross-sectional area normal to the flow [53,66]. Highly dependent on the aspect ratio of the 3-D porous electrodes, neither choice will give a complete description of the system. For this reason, volumetric power density was suggested to be a more sensible criterion [61].

Fundamentally, all electrochemical cells require two electrodes with an ionically conductive electrolyte between them. Moreover, the size of the co-laminar centre channel is usually larger than traditional cell membranes. For this reason, we propose that a volumetric power density normalized by the essential volume of the electrochemical chamber, namely both electrodes and the separating electrolyte, would be the most universally applicable metric for these devices. This harmonization method takes into account any variations in electrolyte channel separation as well as any possible electrode asymmetries (*e.g.*, anode and cathode thickness) with the only assumption being that the inlet/outlet flow field manifolds and other structural support elements are comparable between cells. With this new convention, the key co-laminar flow technologies with the highest power densities reported to date were converted where possible and presented in Table 1. For the sake of comparison, estimates for a typical membrane based vanadium redox battery (VRB) [6,127] and a direct methanol fuel cell (DMFC) [128] are also included.

Due to the considerable differences in testing conditions between the cells presented in Table 1, it is difficult to draw final conclusions about which specific device architecture may be optimal. Factors such as reactant species, reactant and electrolyte concentration, flow rate, temperature, separators, patterned electrodes and the presence of catalysts can all significantly affect the power output of a device. Power density comparisons therefore need to be made with devices benchmarked at standardized conditions. For example, a liquid/liquid co-laminar flow cell could be benchmarked at room temperature with standardized vanadium electrolytes (*e.g.*, 1 M vanadium in 1 M sulphuric acid) and widely available uncatalyzed porous carbon electrodes (*e.g.*, Toray carbon paper). Conducting polarization curve and impedance measurements at a range of flow rates would enable full

Table 1
Performance data on key co-laminar flow cell technologies.

Author (Year)	Category	Electrode type	Fabrication	Additional features	Fuel	Oxidant	Chamber volume (mL)	Flow rate ($\mu L\ min^{-1}$)	Peak power (mW)	Peak power density ($mW\ cm^{-2}$)	Volumetric peak power density ($mW\ cm^{-3}$)
Ferrigno (2002)	Liquid/liquid	Flow-by	Monolithic	None	1 M V^{2+}	1 M VO_2^+	0.0068	1500	3	38	475
							0.0017	42	0.3	4	200
Choban (2005)	Liquid/liquid	Flow-by	Multi-layer	Pt catalysts & mixed media	1 M CH_3OH	Dissolved O_2	0.022	300	3	12	160
Kjeang (2008)	Liquid/liquid	Flow-through	Monolithic	None	2 M V^{2+}	2 M VO_2^+	0.011	300	15	121	1344
							0.011	10	8	70	778
Jayashree (2010)	Liquid/gaseous	Flow-by & air-breathing	Multi-layer	Pt catalyst	1 M HCOOH	Pure O_2	0.045	300	36	55	809
Zebda (2010)	Liquid/liquid	Flow-by	Monolithic	Enzymatic biofuel cell	Glucose	Dissolved O_2	0.001	300	0.03	0.55	19
Lee (2012)	Liquid/liquid	Flow-through	Monolithic	Thin-film current collector	2 M V^{2+}	2 M VO_2^+	0.005	300	11	93	2067
Da Mota (2012)	Liquid/liquid	Flow-by	Multi-layer	Separator & Pt catalysts & patterned electrodes	0.15 M $NaBH_4$	0.5 M cerium ammonium nitrate (CAN)	0.026	3000	135	270	5190
Braff (2013)	Liquid/gaseous	Flow-by & H_2-breathing	Multi-layer	Pt catalyst	Pure H_2	5 M Br_2	0.03	110	199	795	6625
VRB[a]	Liquid/liquid	Flow-through	MEA	Membrane	1.5 M V^{2+}	1.5 M VO_2^+	185	–	130,000	150	700
DMFC[b]	Liquid/gaseous	Flow-through & air-breathing	MEA	Membrane & Pt catalyst	3 M CH_3OH	Pure O_2	0.653	–	450	50	690

[a] VRB MEA dimensions compiled from Skyllas et al. [6] & Zhao et al. [127]. Peak power estimated from upper limits of current density and voltage taken from Zhao et al.
[b] Typical room temperature performance and cell dimensions of DMFC estimated from Xu et al. [128].

characterization of fuel utilization, mass transport and ohmic losses which are inherent to the cell structure and the peak volumetric power density measurements would then enable a direct comparison with other devices.

Despite the variability in testing conditions, some important trends can still be extracted from the data presented in Table 1. For the cells with flow-through porous electrodes, the original cell by Kjeang et al. seemingly leads the cell by Lee et al. when normalized by projected electrode area. When the cross-sectional area of the electrodes are used, however, the cell by Kjeang et al. produces 403 mW cm^{-2} whereas the one by Lee et al. produces 620 mW cm^{-2} at 300 μL min^{-1}. The more universal volumetric power density which takes into account all electrode dimensions accurately captures this performance gain, a direct consequence of the use of gold current collectors to reduce the overall cell resistance. With common vanadium reactants, these cells can also be compared to the flow-by cell originally published by Ferrigno et al. Although the concentrations and flow rates differ, the power output of the flow-through cells is considerably larger than for the flow-by cell, presumably due to the continuous replenishment of reactant at the electrode surface as opposed to the depletion boundary layer which forms at a planar electrode surface. This notion was unambiguously verified in the 2008 study, in which the same electrolyte species were forced to flow either over or through the same porous carbon material, demonstrating that flow-through porous electrodes lead to significant performance gains across a wide range of flow rates [61]. It is also interesting to note that with similar electrode materials and reactant concentrations, co-laminar cells with flow-through electrodes compare quite favourably with and even exceed existing commercial VRB technology, with the question of scale being the crucial difference between the two technologies. With single cell power output in the 10 mW range, the targeted application for co-laminar cells will be quite different from the high-power conventional VRBs with a typical 14-cell stack producing on the order of 1 kW [127]. In summary, recent advances in co-laminar flow cell technology have generated performance levels comparable to more well-established MEA-based cell architectures including direct methanol fuel cells and redox flow batteries, which demonstrates good potential for low-power commercial applications.

Another notable result to appear in recent years is the performance achieved by Da Mota et al. with their co-laminar borohydride fuel cell [108]. In this study it was demonstrated that herringbone grooves, first proposed by Stroock et al. in 2002 to create convective loops enhancing mass transport [129,130], could be imprinted into planar electrodes before platinum deposition. By comparing to a non-patterned baseline, it was shown that the induced chaotic flow doubled the power density from roughly 125 mW cm^{-2} to 250 mW cm^{-2} at 3000 μL min^{-1}. Due to the use of considerably higher flow rates, different reactants with a higher cell potential, mixed media conditions (alkaline anode and acidic cathode), a nitric acid electrolyte that may be consumed during reaction and the presence of catalysts, a direct comparison with the other cells presented in Table 1 is not possible. At least half of the gain in volumetric power density can be attributed to the thinner aspect ratio of the cell with a reduced distance between the electrodes and the reduced volume of the electrodes themselves (here taken to be only the 50 μm groove thickness). Due to the reduced chamber volume and higher flow rates, it is likely that the power lost to pumping was significantly higher than for the other flow cells. As noted in Table 1, this cell used a porous separator to maintain reactant separation during chaotic mixing conditions and was not strictly based on co-laminar flow. Nevertheless, it was reported that the cell compares favourably with high performance conventional membrane-based hydrogen fuel cells, which is a considerable achievement.

The most recent development by Braff et al. also pushes the boundaries for co-laminar cell performance by a considerable margin. In this case, the air-breathing design first proposed by Jayashree et al. was modified so that the cathode would be in contact with the liquid bromine oxidant while the porous anode would harvest electrons from the hydrogen gas fuel. With roughly the same architecture, the performance increase can likely be attributed to the judicious combination of high concentration reactants with fast reaction kinetics and high diffusivity. As with most multilayer designs this cell also takes advantage of graphite current collectors to reduce ohmic losses. Interestingly, all three of the most recent high performance cells in Table 1 utilize some form of highly conductive current collecting electrode. This indicates that co-laminar cell designs have reached sufficient power levels to warrant mitigation of ohmic limitations. In either case, the outstanding performance of these cells further underlines the benefits of the co-laminar flow technology as a precision manufacturing method for smaller scale power applications.

Lastly, the cell by Zebda et al. [37] highlights the importance of co-laminar flow cells in the biofuel cell domain. As the highest efficiency biofuel cell reported at the time of publication, it featured a Y-channel design similar to that of the original cell by Ferrigno et al. Notably, the performance of biofuel cells is predominantly limited by the kinetics of the enzymatically catalysed reactions which are orders of magnitude lower than for non-biological electrocatalysts [131]. That study among others, however, showcases the value of co-laminar flow cells as analytical platforms for testing other technologies such as bio-electrodes.

4.2. Overall utility

Besides performance comparisons based on power, other performance metrics such as fuel utilization, voltage efficiency and Coulombic efficiency are also useful to understand the sources of performance losses but are less commonly available in the literature. These supplementary metrics are increasingly important to consider as the technology progresses. As previously mentioned, architecture modifications are most likely to be tailored towards achieving performance enhancements, whereas fabrication methods are likely to address issues pertaining to cost, device durability and system integration. At the present stage of development, monolithic devices are well-suited to be integrated directly into on-chip applications, while multi-layer devices are poised to become stacked devices for medium-power ($\sim$1–10 W) applications.

Most of the pros and cons of the co-laminar flow technology are known only qualitatively at this stage. The primary advantages are known to be reduced cost and longer durability due to the absence of a membrane, electrolyte pH flexibility and the compatibility with single layer on-chip fabrication. Another significant benefit is the fabrication flexibility of this technology which is amenable to laser etching, CNC machining, lithography, conventional multi-layer MEA fabrication and possibly even 3-D printing. The disadvantages on the other hand are likely to be related to increased ohmic losses due to wider electrode separation, increased sensitivity to pressure fluctuations which would disturb the co-laminar interface, lower recirculation possibilities due to reactant mixing and considerable difficulties with scale-up or stacking of devices. Once these issues have been more firmly assessed, a cost-benefit analysis would reveal whether the co-laminar flow technology is worth pursuing for particular applications.

5. Perspectives

The innovative concept of using co-laminar flow as a replacement for ionomer membranes is generating an increased interest

within the fuel cell research community. A brief search on Web of Knowledge[SM] for "laminar flow" + "fuel cell" reveals that citations have exceeded 500 per year after only a decade of development. In contrast, several other technologies including redox flow batteries and alkaline fuel cells have taken over two decades to generate this level of impact. Although this type of analysis is only approximate, it does reveal that research on co-laminar flow cells is growing relatively quickly. What directions this research takes and whether the results lead to a commercially viable product still remain to be seen. The perspectives offered and the suggestions made in this final section will hopefully accelerate future research to pinpoint the limiting factors for co-laminar flow cells while avoiding redundant studies.

5.1. Research directions

The original design of the co-laminar flow fuel cell has evolved considerably over the past decade. Although the citations for these devices seem to be increasing exponentially, a closer look at the actual number of publications reveals more useful information. The data presented in Fig. 4 accounts for all peer-reviewed scientific publications which report new findings on co-laminar flow based electrochemical cells. In our compilation, the total publications under review are subdivided into those which present new experimental data and those which present strictly modelling results. Review papers and other studies on 'membraneless' fuel cells which rely on flowing electrolytes [132–135] or selective catalysts [136–143] rather than co-laminar flow are not included.

Overall, the number of studies on co-laminar flow cells has increased considerably over the past decade, exceeding twenty per year by the end of 2013. Most of these publications come from well-established research groups that were pioneers in this field. Not indicated in the above publication history, there are however numerous theses and conference presentations available from emerging research groups who are likely to contribute to the future growth of this field. Notably, the proportion of modelling focused publications has varied considerably during the past decade, reaching near parity with experimental results in 2012. A clear majority of these modelling studies simulated various derivatives of the original Y-junction cell with planar flow-by electrode configuration. As demonstrated in the comparison of Table 1, the performance of this original design with planar electrodes has been repeatedly exceeded with more recent designs, thereby reducing the relevance of these modelling studies. Moreover, as mentioned previously, many modelling studies have published reasonable suggestions regarding possible performance enhancements, such as tapering of electrodes or the centre channel, but none of these suggestions have to our knowledge been experimentally verified. Both of these issues indicate a gap between the modelling and experimental approaches which needs to be addressed by groups developing both capabilities in-house, or seeking more collaboration with complementary groups.

According to the old architectural adage form follows function, the proper design of co-laminar flow cells must satisfy certain functional requirements. Occasionally, certain forms fortuitously result in unintended functions coming to light. With colourful reactants such as vanadium ions, the original 2-D planar cell design in clear substrate material allows for excellent visualization of both reduction and oxidation reactions, as can be seen in Fig. 5. This feature allows for easier diagnosis of cell performance issues but has also been utilized in a broader context as well. Combined with the relative ease of fabrication, this visualization feature has allowed microfluidic cells to be used as instructional tools to engage students in the classroom, both in this group and another [144]. Given the advent of 3-D printing with continuously improving resolutions [145], these devices could become even more widespread, making this technology readily accessible to research groups with limited funding who may apply standardized units as a test bed for other electrochemical cell components such as specialized electrodes using immobilized biocatalysts [29] or for detection of microorganism electroactivity [36]. The increasing number of studies such as these indicates that research in co-laminar cells is both expanding and bifurcating into two areas: studies which attempt to modify and improve existing cell designs, and those which use co-laminar flow cells as analytical platforms to investigate other components. In both cases, lessons can be learned with co-laminar flow cells that may have repercussions for other technologies. For instance, whether the herringbone mixers from the study by Da Mota et al. produce co-laminar flow or not, their development was prompted by research on co-laminar flow cells and therefore can be viewed as a useful contribution to the general field of electrochemical energy conversion. In short, in addition to commercial efforts, co-laminar flow cells may come to serve equally important functions as analytical research tools.

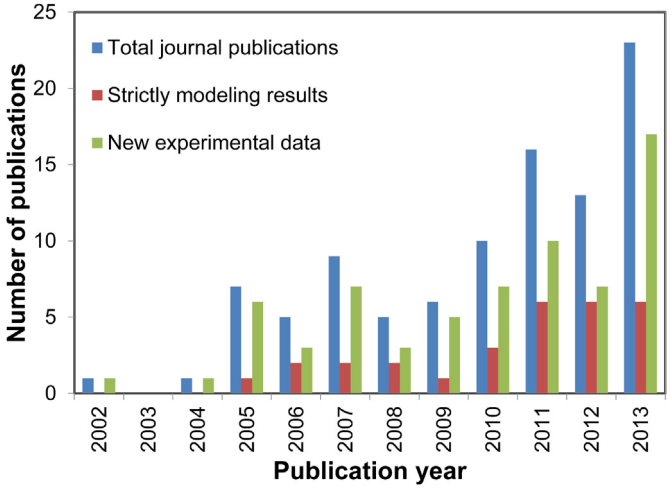

Fig. 4. Peer-reviewed publications related to co-laminar flow cells for electrochemical energy conversion.

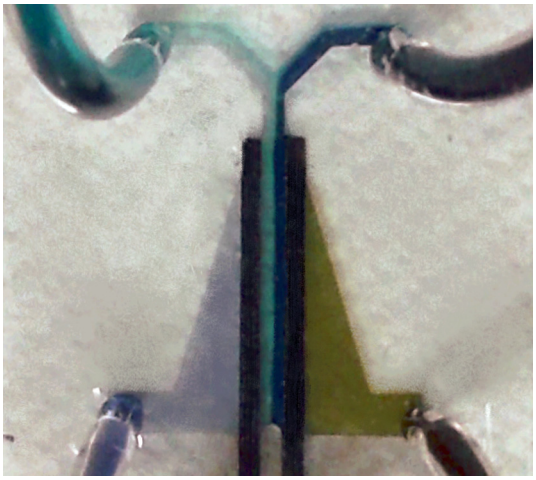

Fig. 5. Real-time image of a monolithic co-laminar flow cell discharging vanadium electrolyte reactants at a flow rate of 5 μL min^{-1} and a potential of 0.3 V. The purple V^{2+} is oxidized to green V^{3+}, whereas the yellow VO_2^+ is reduced to blue VO^{2+} as the reactants flow through the porous carbon electrodes from the inlets at the bottom to the outlets at the top. (For interpretation of the references to colour in this figure legend, the reader is referred to the web version of this article.)

5.2. Technological directions

The central question of commercial viability for co-laminar flow cell technology still remains and can only be assessed by determining which device architecture and electrode structure maximizes the commercial value and benefits of the co-laminar interface. In order to streamline this process, rather than repeating electrochemical investigations on existing fuel and oxidant chemistries that were already performed with larger conventional cells, it would be advantageous to benchmark new cell architectures according to a standard protocol.

Overall, the performance of co-laminar flow cells in terms of power density has already reached or even exceeded the levels of comparable technologies. Performance benchmarks aside, other critical issues related to utility also need to be addressed in order for this technology to become commercially viable, namely the efficiency/fuel utilization, co-laminar interface stability and the stacking/scale-up options. Although nearly 100% fuel utilization has been achieved [61], matching this level of efficiency with high power density has not been accomplished to date. Further research on recirculation may potentially lead to a practical solution in this regard, but more fundamental work on material development and optimization would also be required. Regarding interface stability, few studies have been performed on the effects of pressure fluctuations. Due to the small distances between electrodes and microlitre chamber volumes, it is unlikely that co-laminar cells could withstand pressure fluctuations without the associated performance fluctuations, obviating the need for more quantitative work on this challenge. In terms of capacity increase, there are physical size limits outside of which co-laminar flow is not practical (*cf*. Section 2.1) and scale-up of individual cells is unlikely without the added use of separators [18]. The challenge associated with cell scale-up is perhaps the most pressing technological issue to be addressed by research in this field, and a viable solution would require improved fundamental understanding of two key elements, namely:

1) At what cell dimension and reactant flow rate combinations does co-laminar flow become impractical?
2) What are the power limits for single co-laminar flow cells, and how do they pair with commercial applications?

Establishing reproducible protocols to quantify these points would help to determine the maximum size and power for cells relying strictly on co-laminar flow versus the added use of separators, and would simplify the search for a proper application. Parametric studies such as the one by Thorson et al. [109] which shows that shorter and wider electrodes yield higher current densities, would need to be replicated and expanded with a combined modelling and experimental approach in the context of the design principles outlined in Section 2.1. Scale-up of flow cell systems through stacking or multiplexing is another possible alternative to single cell scale-up. So far, studies involving multiple cells have only considered monolithic planar configurations [16,63,112], thereby achieving a proportionally larger power output at the cost of a considerably larger microfluidic channel area. Sandwich structure fabrication is more amenable to stacking due to the long history of development for conventional fuel cell stacks, and would therefore be the next essential step. Regardless of fabrication method, however, it is necessary to investigate whether maintaining balanced electrolyte pressures will become increasingly challenging for multiple cells at a time.

Whether the above-mentioned challenges can be overcome or not, they also indicate that perhaps a change of perspective is necessary. Perhaps the true challenge for co-laminar flow cells is the question of proper application matching and system integration. Finding a stable or stationary low-power commercial application to drive research in this field would likely require minimal stacking and no special pressure control. One of the most suitable applications identified to date may be the wireless sensor networks used in remote locations which would benefit considerably from the relatively low cost and minimal maintenance of co-laminar flow cells [146]. Another promising application of this technology is for simultaneous cooling and powering of microelectronics. A recently launched collaborative project between IBM and Ecole Polytechnique Fédérale de Lausanne (EPFL) is investigating the prospects for using on-chip co-laminar redox flow cells to power and cool multiprocessor systems, an application for which they claim this technology may have a beneficially disruptive effect [147]. In order for such projects to achieve practical and cost-effective functionality, research needs to be conducted at the entire microfluidic system level which includes reservoirs, manifolds, and efficient pumping of reactants. Such a wide scope can only be achieved through collaboration within the microfluidics community.

6. Conclusions

In this review, we have summarized the key developments in the evolution of 'membraneless' microfluidic electrochemical cells which utilize co-laminar flow to minimize reactant crossover and mixing. Some of the more notable performance related highlights include the use of flow-through porous electrodes for greater electrochemically active surface area, the combination of patterned electrodes with porous separators for improved mass transport, the addition of current collectors for reducing ohmic losses, and the strategic use of high concentration reactants with high diffusivity. These enhancements have produced cells with power densities surpassing those of previous co-laminar flow cells and even conventional electrochemical flow cell technologies and have expanded the functionality of the co-laminar flow technology to include rechargeable battery operation. In regards to cell design and utility, two important trends were identified, namely multi-layer sandwich structures showing potential for stacked operation and medium-power applications and single-layer monolithic construction for low-power on-chip applications. From a simple analysis of historical trends, the research in this field was shown to increase similarly to conventional electrochemical energy conversion technologies in part due to its adoption as a practical analytical tool for multi-physics simulations and lab-scale experiments particularly in the biofuel cell community. Once the right commercial application has been determined, device integration would be the next logical step for the co-laminar flow cell technology. It is hoped that the present review will aid research in this field to address the remaining challenges for commercial utility.

Acknowledgements

Funding for this research provided by the Natural Sciences and Engineering Research Council of Canada, Western Economic Diversification Canada, Canada Foundation for Innovation, British Columbia Knowledge Development Fund, and Simon Fraser University (SFU) is highly appreciated. The authors express sincere thanks to Spencer Arbour for assistance with graphics.

References

[1] J. Morse, Int. J. Energy Res. 31 (2007) 576–602.
[2] A.J. Bard, L.R. Faulkner, in: Electrochemical Methods: Fundamentals and Applications, second ed., John Wiley & Sons Inc., 2001.

[3] M.M. Mench, Fuel Cell Engines, John Wiley & Sons Inc., 2008.
[4] Z. Yang, J. Zhang, M.C.W. Kintner-Meyer, X. Lu, D. Choi, J.P. Lemmon, J. Liu, Chem. Rev. 111 (2011) 3577–3613.
[5] C. Garcia, B. Chang, D. Johnson, in: NHA Annu. Hydrog. Conf., 2006 pp. NASA/TM-2006-214054.
[6] M. Skyllas-Kazacos, M.H. Chakrabarti, S.A. Hajimolana, F.S. Mjalli, M. Saleem, J. Electrochem. Soc. 158 (2011) R55–R79.
[7] S.J. Peighambardoust, S. Rowshanzamir, M. Amjadi, Int. J. Hydrogen Energy 35 (2010) 9349–9384.
[8] H. Vafiadis, M. Skyllas-Kazacos, J. Memb. Sci. 279 (2006) 394–402.
[9] R. Borup, J. Meyers, B. Pivovar, Y.S. Kim, R. Mukundan, N. Garland, D. Myers, M. Wilson, F. Garzon, D. Wood, P. Zelenay, K. More, K. Stroh, T. Zawodzinski, J. Boncella, J.E. McGrath, M. Inaba, K. Miyatake, M. Hori, K. Ota, Z. Ogumi, S. Miyata, A. Nishikata, Z. Siroma, Y. Uchimoto, K. Yasuda, K. Kimijima, N. Iwashita, Chem. Rev. 107 (2007) 3904–3951.
[10] M. Skyllas-Kazacos, M. Kazacos, J. Power Sources 196 (2011) 8822–8827.
[11] E.H. Yu, X. Wang, U. Krewer, L. Li, K. Scott, Energy Environ. Sci. 5 (2012) 5668–5680.
[12] M.A. Burns, B.N. Johnson, S.N. Brahmasandra, K. Handique, J.R. Webster, M. Krishnan, T.S. Sammarco, P.M. Man, D. Jones, D. Heldsinger, C.H. Mastrangelo, D.T. Burke, Science 282 (80) (1998) 484–487.
[13] S. Takayama, E. Ostuni, P. LeDuc, K. Naruse, D.E. Ingber, G.M. Whitesides, Nature 411 (2001) 1016.
[14] R.F. Ismagilov, T.D. Rosmarin, P.J.A. Kenis, D.T. Chiu, W. Zhang, H.A. Stone, G.M. Whitesides, Anal. Chem. 73 (2001) 4682–4687.
[15] G.M. Whitesides, Nature 442 (2006) 368–373.
[16] R. Ferrigno, A.D. Stroock, T.D. Clark, M. Mayer, G.M. Whitesides, J. Am. Chem. Soc. 124 (2002) 12930–12931.
[17] E.R. Choban, L.J. Markoski, A. Wieckowski, P.J.A. Kenis, J. Power Sources 128 (2004) 54–60.
[18] E. Kjeang, N. Djilali, D. Sinton, J. Power Sources 186 (2009) 353–369.
[19] S.A. Mousavi Shaegh, N.-T. Nguyen, S.H. Chan, Int. J. Hydrogen Energy 36 (2011) 5675–5694.
[20] B. Ho, E. Kjeang, Cent. Eur. J. Eng. 1 (2011) 123–131.
[21] R. Byron Bird, W.E. Stewart, E.N. Lightfoot, Transport Phenomena, second ed., John Wiley & Sons Ltd, 2001.
[22] A. Einstein, Investigations on the Theory of the Brownian Movement, second ed., Dover Publications, 1956.
[23] S. Tominaka, H. Obata, T. Osaka, Energy Environ. Sci. 2 (2009) 845–848.
[24] R.K. Arun, W. Bekele, A. Ghatak, Electrochim. Acta 87 (2013) 489–496.
[25] F.M. Cuevas-Muñiz, M. Guerra-Balcázar, F. Castaneda, J. Ledesma-García, L.G. Arriaga, J. Power Sources 196 (2011) 5853–5857.
[26] S. Hasegawa, K. Shimotani, K. Kishi, H. Watanabe, Electrochem. Solid-State Lett. 8 (2005) A119–A121.
[27] E. Kjeang, B. Proctor, A. Brolo, D.A. Harrington, N. Djilali, D. Sinton, Electrochim. Acta 52 (2007) 4942–4946.
[28] E. Kjeang, A.G. Brolo, D.A. Harrington, N. Djilali, D. Sinton, J. Electrochem. Soc. 154 (2007) B1220–B1226.
[29] Z. Li, Y. Zhang, P.R. LeDuc, K.B. Gregory, Biotechnol. Bioeng. 108 (2011) 2061–2069.
[30] K.G. Lim, G.T.R. Palmore, Biosens. Bioelectron. 22 (2007) 941–947.
[31] P.O. López-Montesinos, N. Yossakda, A. Schmidt, F.R. Brushett, W.E. Pelton, P.J.A. Kenis, J. Power Sources 196 (2011) 4638–4645.
[32] D. Morales-Acosta, M.D. Morales-Acosta, L.A. Godinez, L. Álvarez-Contreras, S.M. Duron-Torres, J. Ledesma-García, L.G. Arriaga, J. Power Sources 196 (2011) 9270–9275.
[33] J.-C. Shyu, C.-L. Huang, J. Power Sources 196 (2011) 3233–3238.
[34] J.-C. Shyu, C.-S. Wei, C.-J. Lee, C.-C. Wang, Appl. Therm. Eng. 30 (2010) 1863–1871.
[35] M.H. Sun, G. Velve Casquillas, S.S. Guo, J. Shi, H. Ji, Q. Ouyang, Y. Chen, Microelectron. Eng. 84 (2007) 1182–1185.
[36] H.-Y. Wang, J.-Y. Su, Bioresour. Technol. 145 (2013) 271–274.
[37] A. Zebda, L. Renaud, M. Cretin, C. Innocent, R. Ferrigno, S. Tingry, Sensors Actuat. B Chem. 149 (2010) 44–50.
[38] A. Zebda, L. Renaud, M. Cretin, F. Pichot, C. Innocent, R. Ferrigno, S. Tingry, Electrochem. Commun. 11 (2009) 592–595.
[39] E.R. Choban, J.S. Spendelow, L. Gancs, A. Wieckowski, P.J.A. Kenis, Electrochim. Acta 50 (2005) 5390–5398.
[40] E.R. Choban, P. Waszczuk, P.J.A. Kenis, Electrochem. Solid-State Lett. 8 (2005) A348.
[41] J.L. Cohen, D.A. Westly, A. Pechenik, H.D. Abruña, J. Power Sources 139 (2005) 96–105.
[42] J.L. Cohen, D.J. Volpe, D.A. Westly, A. Pechenik, H.D. Abruña, Langmuir 21 (2005) 3544–3550.
[43] A. Déctor, F.M. Cuevas-Muñiz, M. Guerra-Balcázar, L. a. Godínez, J. Ledesma-García, L.G. Arriaga, Int. J. Hydrogen Energy (2013) 1–6.
[44] A. Déctor, J.P. Esquivel, M.J. González, M. Guerra-Balcázar, J. Ledesma-García, N. Sabaté, L.G. Arriaga, Electrochim. Acta 92 (2013) 31–35.
[45] R. Galindo, A. Dector, L.G. Arriaga, S. Gutiérrez, P. Herrasti, J. Electroanal. Chem. 671 (2012) 38–43.
[46] A. Li, S.H. Chan, N.-T. Nguyen, J. Micromech. Microeng. 17 (2007) 1107–1113.
[47] D. Morales-Acosta, H. Rodríguez, G. Luis, A. Godinez, L.G. Arriaga, J. Power Sources 195 (2010) 1862–1865.
[48] I.B. Sprague, P. Dutta, S. Ha, Proc. Inst. Mech. Eng. Part A J. Power Energy 223 (2009) 799–808.
[49] S.K. Yoon, G.W. Fichtl, P.J.A. Kenis, Lab. Chip 6 (2006) 1516–1524.
[50] A.S. Hollinger, P.J.A. Kenis, J. Power Sources 240 (2013) 486–493.
[51] R.S. Jayashree, L. Gancs, E.R. Choban, A. Primak, D. Natarajan, L.J. Markoski, P.J.A. Kenis, J. Am. Chem. Soc. 127 (2005) 16758–16759.
[52] S.A. Mousavi Shaegh, N.-T. Nguyen, S.H. Chan, J. Micromech. Microeng. 20 (2010) 105008.
[53] S.A. Mousavi Shaegh, N.-T. Nguyen, S.H. Chan, W. Zhou, Int. J. Hydrogen Energy 37 (2012) 3466–3476.
[54] R.S. Jayashree, S.K. Yoon, F.R. Brushett, P.O. Lopez-Montesinos, D. Natarajan, L.J. Markoski, P.J.A. Kenis, J. Power Sources 195 (2010) 3569–3578.
[55] R.S. Jayashree, D. Egas, J.S. Spendelow, D. Natarajan, L.J. Markoski, P.J.A. Kenis, Electrochem. Solid-State Lett. 9 (2006) A252–A256.
[56] F.R. Brushett, R.S. Jayashree, W.-P. Zhou, P.J.A. Kenis, Electrochim. Acta 54 (2009) 7099–7105.
[57] S.A. Mousavi Shaegh, N.-T. Nguyen, S.H. Chan, J. Power Sources 209 (2012) 312–317.
[58] D.T. Whipple, R.S. Jayashree, D. Egas, N. Alonso-Vante, P.J.A. Kenis, Electrochim. Acta 54 (2009) 4384–4388.
[59] C. Chen, P. Yang, J. Power Sources 123 (2003) 37–42.
[60] G. Girishkumar, B. McCloskey, A.C. Luntz, S. Swanson, W. Wilcke, J. Phys. Chem. Lett. 1 (2010) 2193–2203.
[61] E. Kjeang, R. Michel, D.A. Harrington, N. Djilali, D. Sinton, J. Am. Chem. Soc. 130 (2008) 4000–4006.
[62] D. Fuerth, A. Bazylak, J. Fluids Eng. 135 (2013) 021102.
[63] B. Ho, E. Kjeang, J. Fluids Eng. 135 (2013) 021304.
[64] E. Kjeang, R. Michel, D.A. Harrington, D. Sinton, N. Djilali, Electrochim. Acta 54 (2008) 698–705.
[65] J.W. Lee, E. Kjeang, Int. J. Hydrogen Energy 37 (2012) 9359–9367.
[66] J.W. Lee, E. Kjeang, J. Power Sources 242 (2013) 472–477.
[67] S. Moore, D. Sinton, D. Erickson, J. Power Sources 196 (2011) 9481–9487.
[68] K.S. Salloum, J.R. Hayes, C.A. Friesen, J.D. Posner, J. Power Sources 180 (2008) 243–252.
[69] J.W. Lee, M.-A. Goulet, E. Kjeang, Lab. Chip 13 (2013) 2504–2507.
[70] M.N. Nasharudin, S.K. Kamarudin, U.A. Hasran, M.S. Masdar, Int. J. Hydrogen Energy 39 (2014) 1039–1055.
[71] A. Bazylak, D. Sinton, N. Djilali, J. Power Sources 143 (2005) 57–66.
[72] W. Chen, F. Chen, J. Power Sources 162 (2006) 1137–1146.
[73] M.-H. Chang, F. Chen, N.-S. Fang, J. Power Sources 159 (2006) 810–816.
[74] F. Chen, M.-H. Chang, C.-W. Hsu, Electrochim. Acta 52 (2007) 7270–7277.
[75] J. Lee, K.G. Lim, G.T.R. Palmore, A. Tripathi, Anal. Chem. 79 (2007) 7301–7307.
[76] F. Chen, M.-H. Chang, M.-K. Lin, Electrochim. Acta 52 (2007) 2506–2514.
[77] D.H. Ahmed, H.B. Park, H.J. Sung, J. Power Sources 185 (2008) 143–152.
[78] J. Phirani, S. Basu, J. Power Sources 175 (2008) 261–265.
[79] H.B. Park, D.H. Ahmed, K.H. Lee, H.J. Sung, Electrochim. Acta 54 (2009) 4416–4425.
[80] A. Ebrahimi Khabbazi, A.J. Richards, M. Hoorfar, J. Power Sources 195 (2010) 8141–8151.
[81] D.H. Ahmed, H.B. Park, Int. J. Energy Res. 34 (2010) 878–896.
[82] I.B. Sprague, D. Byun, P. Dutta, Electrochim. Acta 55 (2010) 8579–8589.
[83] W.A. Braff, C.R. Buie, ECS Trans. 33 (2011) 179–190.
[84] J. Xuan, D.Y.C. Leung, M.K.H. Leung, M. Ni, H. Wang, Int. J. Hydrogen Energy 36 (2011) 9231–9241.
[85] J. Xuan, M.K.H. Leung, D.Y.C. Leung, M. Ni, H. Wang, Int. J. Hydrogen Energy 36 (2011) 11075–11084.
[86] I. Sprague, P. Dutta, Electrochim. Acta 56 (2011) 4518–4525.
[87] J. Xuan, D.Y.C. Leung, M.K.H. Leung, H. Wang, M. Ni, J. Power Sources 196 (2011) 9391–9397.
[88] H. Wang, D.Y.C. Leung, J. Xuan, Int. J. Hydrogen Energy 36 (2011) 14704–14718.
[89] I.B. Sprague, P. Dutta, Numer. Heat. Transf. Part A Appl. 59 (2011) 1–27.
[90] D. Krishnamurthy, E.O. Johansson, J.W. Lee, E. Kjeang, J. Power Sources 196 (2011) 10019–10031.
[91] R. Hassanshahi, M. Fathipour, M. Feali, Int. J. Adv. Renew. Energy Res. 1 (2012) 605–610.
[92] J. Xuan, M.K.H. Leung, D.Y.C. Leung, H. Wang, Appl. Energy 90 (2012) 87–93.
[93] I. Sprague, P. Dutta, SIAM J. Appl. Math. 72 (2012) 1149–1168.
[94] C.-F. Flores-Rivera, ISRN Appl. Math. 2012 (2012) 1–24.
[95] J. Peng, Z.Y. Zhang, H.T. Niu, Fuel Cells 12 (2012) 1009–1018.
[96] J. Xuan, M.K.H. Leung, D.Y.C. Leung, H. Wang, Appl. Energy 90 (2012) 80–86.
[97] R. Hassanshahi, M. Fathipour, Int. J. Adv. Renew. Energy Res. 1 (2012) 649–654.
[98] W. Huo, Y. Zhou, H. Zhang, Int. J. Electrochem. Sci. 8 (2013) 4827–4838.
[99] H. Zhang, J. Xuan, H. Xu, M.K.H. Leung, D.Y.C. Leung, L. Zhang, H. Wang, L. Wang, Appl. Energy (2013) 1–7.
[100] J. Xuan, H. Wang, D.Y.C. Leung, M.K.H. Leung, H. Xu, L. Zhang, Y. Shen, J. Power Sources 231 (2013) 1–5.
[101] H. Zhang, M.K.H. Leung, J. Xuan, H. Xu, L. Zhang, D.Y.C. Leung, H. Wang, Int. J. Hydrogen Energy 38 (2013) 6526–6536.
[102] I.B. Sprague, P. Dutta, Electrochim. Acta 91 (2013) 20–29.
[103] J. Xuan, D.Y.C. Leung, H. Wang, M.K.H. Leung, B. Wang, M. Ni, Appl. Energy 104 (2013) 400–407.
[104] R.A. García-Cuevas, I. Cervantes, L.G. Arriaga, I.A. Diaz-Diaz, Int. J. Hydrogen Energy 38 (2013) 14791–14800.
[105] H.B. Park, K.H. Lee, H.J. Sung, J. Power Sources 226 (2013) 266–271.

[106] E. Kjeang, J. McKechnie, D. Sinton, N. Djilali, J. Power Sources 168 (2007) 379–390.
[107] A.S. Hollinger, R.J. Maloney, R.S. Jayashree, D. Natarajan, L.J. Markoski, P.J.A. Kenis, J. Power Sources 195 (2010) 3523–3528.
[108] N. Da Mota, D.A. Finkelstein, J.D. Kirtland, C.A. Rodriguez, A.D. Stroock, H.D. Abruña, J. Am. Chem. Soc. 134 (2012) 6076–6079.
[109] M.R. Thorson, F.R. Brushett, C.J. Timberg, P.J.A. Kenis, J. Power Sources 218 (2012) 28–33.
[110] X. Zhu, B. Zhang, D.-D. Ye, J. Li, Q. Liao, J. Power Sources 247 (2014) 346–353.
[111] M. Guerra-Balcázar, F.M. Cuevas-Muñiz, F. Castaneda, R. Ortega, L. Álvarez-Contreras, J. Ledesma-García, L.G. Arriaga, Electrochim. Acta 56 (2011) 8758–8762.
[112] K.S. Salloum, J.D. Posner, J. Power Sources 196 (2011) 1229–1234.
[113] E. Kjeang, in: Next Gener. Batter., 2013. Boston, MA.
[114] M.-A. Goulet, E. Kjeang, Electrochim. Acta (2014). ISE13-04c-02, accepted manuscript.
[115] W.A. Braff, C.R. Buie, M.Z. Bazant, J. Electrochem. Soc. 160 (2013) A2056–A2063.
[116] W.A. Braff, M.Z. Bazant, C.R. Buie, Nat. Commun. 4 (2013) 2346.
[117] A.S. Gago, D. Morales-Acosta, L.G. Arriaga, N. Alonso-Vante, J. Power Sources 196 (2011) 1324–1328.
[118] J. Ma, A.S. Gago, N. Alonso-Vante, J. Electrochem. Soc. 160 (2013) F859–F866.
[119] K.S. Salloum, J.D. Posner, J. Power Sources 195 (2010) 6941–6944.
[120] A. Zebda, L. Renaud, M. Cretin, C. Innocent, F. Pichot, R. Ferrigno, S. Tingry, J. Power Sources 193 (2009) 602–606.
[121] M.J. González-Guerrero, J.P. Esquivel, D. Sánchez-Molas, P. Godignon, F.X. Muñoz, F.J. Del Campo, F. Giroud, S.D. Minteer, N. Sabaté, Lab. Chip (2013) 2972–2979.
[122] T. Beneyton, I.P.M. Wijaya, C. Ben Salem, A.D. Griffiths, V. Taly, Chem. Commun. (Camb.) 49 (2013) 1094–1096.
[123] D. Ye, Y. Yang, J. Li, X. Zhu, Q. Liao, B. Deng, R. Chen, Int. J. Hydrogen Energy (2013) 1–6.
[124] B. Bauer, H. Strathmann, F. Effenberger, Desalination 79 (1990) 124–144.
[125] J.I. Hur, D.D. Meng, C.-J. Kim, J. Microelectromech. Syst. 21 (2012) 476–483.
[126] J. Larminie, A. Dicks, Fuel Cell Systems Explained, in: second ed. (Ed.), John Wiley & Sons Ltd, 2003.
[127] P. Zhao, H. Zhang, H. Zhou, J. Chen, S. Gao, B. Yi, J. Power Sources 162 (2006) 1416–1420.
[128] C. Xu, A. Faghri, X. Li, T. Ward, Int. J. Hydrogen Energy 35 (2010) 1769–1777.
[129] J.D. Kirtland, C.R. Siegel, A.D. Stroock, New J. Phys. 11 (2009) 075028.
[130] A.D. Stroock, S.K.W. Dertinger, A. Ajdari, I. Mezic, H.A. Stone, G.M. Whitesides, Science 295 (80) (2002) 647–651.
[131] F. Gao, L. Viry, M. Maugey, P. Poulin, N. Mano, Nat. Commun. 1 (2010) 1–7.
[132] F.R. Brushett, H.T. Duong, J.W. Ng, R.L. Behrens, A. Wieckowski, P.J.A. Kenis, J. Electrochem. Soc. 157 (2010) B837–B845.
[133] F.R. Brushett, M.S. Naughton, J.W.D. Ng, L. Yin, P.J.A. Kenis, Int. J. Hydrogen Energy 37 (2012) 2559–2570.
[134] H.-R. Jhong, F.R. Brushett, L. Yin, D.M. Stevenson, P.J.A. Kenis, J. Electrochem. Soc. 159 (2012) B292–B298.
[135] M.S. Naughton, F.R. Brushett, P.J.A. Kenis, J. Power Sources 196 (2011) 1762–1768.
[136] C.M. Moore, S.D. Minteer, R.S. Martin, Lab. Chip 5 (2005) 218–225.
[137] S.A. Mousavi Shaegh, N.-T. Nguyen, S.M. Mousavi Ehteshami, S.H. Chan, Energy Environ. Sci. 5 (2012) 8225–8228.
[138] A.K. Shukla, R.K. Raman, K. Scott, Fuel Cells 5 (2005) 436–447.
[139] W. Sung, J.-W. Choi, J. Power Sources 172 (2007) 198–208.
[140] M. Togo, A. Takamura, T. Asai, H. Kaji, M. Nishizawa, Electrochim. Acta 52 (2007) 4669–4674.
[141] M. Togo, A. Takamura, T. Asai, H. Kaji, M. Nishizawa, J. Power Sources 178 (2008) 53–58.
[142] S. Tominaka, S. Ohta, H. Obata, T. Momma, T. Osaka, J. Am. Chem. Soc. 130 (2008) 10456–10457.
[143] S. Topcagic, S.D. Minteer, Electrochim. Acta 51 (2006) 2168–2172.
[144] K. Davis, J. Muskin, Mater. Res. Soc. Symp. Proc. 1320 (2011).
[145] T. Serra, J.A. Planell, M. Navarro, Acta Biomater. 9 (2012) 5521–5530.
[146] W. Gellett, M. Kesmez, J. Schumacher, N. Akers, S.D. Minteer, Electroanalysis 22 (2010) 727–731.
[147] M.M. Sabry, A. Sridhar, D. Atienza, P. Ruch, B. Michel, in: Proc. IEEE/ACM 2014 Des. Autom. Test Eur. Conf., 2014, pp. 70–75.